Supporting Online Material

Materials and Methods

Growth conditions

S. cerevisiae was grown at 30°C, and all other strains were grown at 25°C on standard *S. cerevisiae* plate or liquid media (e.g., YPD and SC).

dsRNA enrichment

Double-stranded RNA was enriched as described (*8*), with some modifications. Total RNA was isolated by standard hot-phenol extraction from saturated YPD cultures and treated with DNase I (Ambion). Ribosomal RNA integrity and the accuracy of RNA quantification were confirmed on agarose gels stained with ethidium bromide. 100 µg total RNA was incubated in 2.8 M LiCl overnight at –20°C in a volume of 80 µl to allow most cellular transcripts to precipitate. After centrifugation, the supernatant was collected, and dsRNA was precipitated using 0.1 volume 3 M NaCl and 2.5 volumes of ethanol. Resuspended RNA was analyzed on 1% agarose gels stained with ethidium bromide.

Killer plate assay

Killing and immunity were qualitatively estimated on methylene-blue agar plates (MBA, pH 4.5) as previously described (*9*). For Figure 1A, frozen stocks of the strains were streaked out on YPD plates and grown at 30°C for two days. Single colonies were then used to inoculate YPD liquid cultures. After overnight growth at 30°C, ~200 cells were plated on YPD plates and grown to colony size at 30°C. Colonies were replica-plated on MBA plates that had been seeded with an overlay of a sensitive *S. cerevisiae* strain (*7*) and incubated at 23°C for 2–3 days. Killing can be detected as a clear halo surrounding the colony.

RNA blots

1 µg of total, DNase-treated RNA isolated from saturated cultures was treated with glyoxal using NorthernMax-Gly Sample Loading Dye (Ambion). The samples were loaded on a 1% agarose gel prepared using NorthernMax-Gly Gel Running Buffer (Ambion) according to the manufacturer's instructions. The RNA was blotted onto a Nytran membrane in 20X SSC (175.3 g NaCl, 88.2 g sodium citrate in 1.0 l water adjusted to pH 7) using the TurboBlotter System (Whatman). After UV crosslinking RNA to the membrane, glyoxal treatment was reversed by incubating the membrane in 10 mM Tris-HCl pH 8 for 20 minutes at room temperature. The membrane was incubated in 12 ml QuickHyb solution (Stratagene) with 1.0 mg salmon-sperm ssDNA (Sigma) for 1 hour at 65°C, and then radio-labeled RNA probe was added. After an overnight hybridization at 65°C, the membrane was washed twice in 2X SSC, 0.1% SDS for 5 minutes and once in 0.2X SSC, 0.1% SDS for 30 minutes. The membrane was exposed to phosphorimager plates and analyzed using the Bass Phosphorimager system (Fuji Film). To generate templates for the RNA probes, yeast RNA was reverse transcribed and amplified (*ACT1* forward primer, `CGTCGGTAGACCAAGACACC`; *ACT1*-T7 reverse primer, `TTCTAATACGACTCACTATAGGGAGAAAGAGTAACCACGTTCACT`; *L-A* mRNA forward primer,

CTGATCGCGGAACTTTTGTT; *L-A*-T7 mRNA reverse primer,
TTCTAATACGACTCACTATAGGTAGTTGTGCCGAAGCCTGT; *L-BC* mRNA forward primer,
TTCTAGGGTCCAATATGGCTTT; *L-BC*-T7 mRNA reverse primer,
TTCTAATACGACTCACTATAGGGGCACATCCTCTTCTGGAAA). The amplified products were gel-purified and used for *in vitro* transcription using MegaScript Kit (Ambion) with 5 µl of [α-^{32}P]UTP (800 Ci/mmol) according to the manufacturer's instructions.

Small-RNA sequencing and analysis

Total RNA was isolated using hot phenol from log-phase YPD cultures of DPB249 (WT) and DPB258 (+*AGO1, DCR1*), and small-RNA cDNA libraries were prepared as described (*10*) for sequencing using the Illumina SBS platform. After removing the adaptor sequences, reads representing the small RNAs were collapsed to a non-redundant set, and 14–30-nt sequences were mapped to the W303 and S288C genomes, the *S. castellii AGO1* and *DCR1* genes, and the viral and satellite element genomes, allowing no mismatches and recovering all hits (table S1). When counting the reads matching a locus, the count was hit-normalized, i.e., normalized to the number of times that a small-RNA sequence matched the genome. For example, a small RNA sequenced twice that mapped to the genome five times contributed 0.4 read counts to each genomic locus. Sequence and feature files for *S. cerevisiae* W303 and *S. cerevisiae* S288C were obtained from the Saccharomyces Genome Resequencing Project (SGRP, in June 2009) and from the *Saccharomyces* Genome Database (SGD, on September 10, 2007), respectively. Because the Ty and Y′ genomic sequences were not complete in the W303 genome file, read densities for those elements were calculated based on the sequences in the S288C genome file. All other mappings and analyses were performed using the W303 genome file and annotations. To minimize annotation quality differences between *S. cerevisiae* and *S. castellii*, only *S. cerevisiae* genes that were part of the YGOB (Version 4) were considered.

Strand-specific RNA-Seq

Cultures of DPB249 (WT), DPB252 (+*AGO1),* DPB255 (+*DCR1*) and DPB258 (+*AGO1, DCR1*) were grown in YPD to OD_{600} 0.6–0.8, and poly(A)-selected RNA was fragmented and sequenced as described (*1*). The first 25 nt of each 36-nt read was isolated and collapsed into a non-redundant set of 25-nt sequences, recording the number of reads representing each sequence (table S2). Sequences were mapped as done for the small-RNA sequences, allowing no mismatches and recovering all hits. For comparison between libraries, the number of reads was normalized by the number of total genome-matching reads, excluding those that matched tRNA and rRNA to prevent skewing of the normalization by differences in poly(A) enrichment efficiencies.

mRNA dataset

The 5′ and 3′ boundaries of *S. castellii* mRNA transcripts were previously determined using RNA-Seq data (*1*); to facilitate comparisons to *S. castellii*, the same computational algorithm was applied to the *S. cerevisiae* mRNAs, using the same number and complexity of genome-matching RNA-Seq tags (excluding tRNA and rRNA matches). Of 5505 annotated ORFs in the YGOB, 4484 had RNA-Seq tags mapping to at least 70% of the ORF nucleotides and were suitable for this transcript-extension protocol. In figure S3, figure S5A, C and D, and figure S6, the remaining 1021 ORFs were added to the mRNA set and included in the analyses without considering their UTRs.

DNA sequencing and analysis

Total DNA was isolated from *Z. bailii* and *H. uvarum* by phenol extraction. After RNase-treatment, the DNA was sonicated to a fragment size of ~600 bp and prepared for sequencing using the Illumina Genomic DNA sample-prep kit. Assembly was with EDENA (*11*), considering the first 30 nt of each read, using 20 nt as the minimum overlap length and allowing no mismatches or end-trimming of the resulting contigs. Contigs longer than 80 nt were used for further analyses. As a control, *S. castellii* was sequenced, and contigs were analyzed in parallel to those of the newly sequenced genomes. To simulate the potentially lower coverage of the *H. uvarum* genome, 1000 cohorts were randomly generated to each include 45% of the *S. castellii* sequences (a percentage chosen to simulate the fraction of conserved proteins identified in the *H. uvarum* contigs).

Phylogenetic analysis

For the fungal phylogenetic analysis in Figure 1B, the sequences of large ribosomal subunits (LSU) were obtained from The European Ribosomal Database (http://bioinformatics.psb.ugent.be/webtools/rRNA/index.html). The ID of the sequences were as follows: *C. neoformans* L14067*, S. pombe* Z19136*, S. japonicus* Z32848*, Magnaporthe grisea* AB026819*, C. albicans* L07796, *S. cerevisiae* 2U53879. In addition, LSU sequences were obtained from GenBank with the following accession numbers: *S. castellii* AY048167*, S. bayanus* AY048156*, S. paradoxus* FN868260, *S. mikatae* AF399762*, U. hordei* AF453934 and *U. maydis* DQ025485. The sequences were aligned using ClustalW and a ML tree was constructed by running DNAML (PHYLIP) on the alignment. Additional species were added to the tree consistent with published topological orders and by inferring their branch lengths from those phylogenetic analyses (*12*, *13*).

Supplemental References

1. I. A. Drinnenberg *et al*., RNAi in budding yeast. *Science* **326,** 544 (2009); 10.1126/science.1176945.
2. R. B. Wickner, Double-stranded RNA viruses of *Saccharomyces cerevisiae*. *Microbiol. Rev.* **60**, 250 (1996).
3. M. J. Schmitt, F. Breinig, Yeast viral killer toxins: Lethality and self-protection. *Nat. Rev. Microbiol.* **4**, 212 (2006).
4. S. W. Ding, O. Voinnet, Antiviral immunity directed by small RNAs. *Cell* **130**, 413 (2007).
5. G. I. Naumov, IuV. Ivannikoiva, E. S. Naumova, [Molecular polymorphism of viral dsRNA of yeast *Saccharomyces paradoxus*]. *Mol. Gen. Mikrobiol. Virusol.* **2005**, 38 (2005).
6. Y. V. Ivannikova, E. S. Naumova, G. I. Naumov, Viral dsRNA in the wine yeast *Saccharomyces bayanus* var. *uvarum*. *Res. Microbiol.* **158**, 638 (2007).
7. R. P. Valle, R. B. Wickner, Elimination of L-A double-stranded RNA virus of *Saccharomyces cerevisiae* by expression of gag and gag-pol from an L-A cDNA clone. *J. Virol.* **67**, 2764 (1993).
8. H. M. Fried, G. R. Fink, Electron microscopic heteroduplex analysis of "killer" double-stranded RNA species from yeast. *Proc. Natl. Acad. Sci. U S A* **75**, 4224 (1978).
9. M. J. Schmitt, D. J. Tipper, K28, a unique double-stranded RNA killer virus of *Saccharomyces cerevisiae*. *Mol. Cell. Biol.* **10**, 4807 (1990).
10. A. Grimson *et al.*, Early origins and evolution of microRNAs and Piwi-interacting RNAs in animals. *Nature* **455**, 1193 (2008).
11. D. Hernandez, P. Francois, L. Farinelli, M. Osteras, J. Schrenzel, De novo bacterial genome sequencing: Millions of very short reads assembled on a desktop computer. *Genome Res.* **18**, 802 (2008).
12. C. P. Kurtzman, C. J. Robnett, Phylogenetic relationships among yeasts of the 'Saccharomyces complex' determined from multigene sequence analyses. *FEMS Yeast Res.* **3**, 417 (2003).
13. D. A. Fitzpatrick, M. E. Logue, J. E. Stajich, G. Butler, A fungal phylogeny based on 42 complete genomes derived from supertree and combined gene analysis. *BMC Evol. Biol.* **6**, 99 (2006).
14. S. M. Hedtke, T. M. Townsend, D. M. Hillis, Resolution of phylogenetic conflict in large data sets by increased taxon sampling. *Syst. Biol.* **55**, 522 (2006).
15. H. Nakayashiki, N. Kadotani, S. Mayama, Evolution and diversification of RNA silencing proteins in fungi. *J. Mol. Evol.* **63**, 127 (2006).
16. J. D. Laurie, R. Linning, G. Bakkeren, Hallmarks of RNA silencing are found in the smut fungus *Ustilago hordei* but not in its close relative *Ustilago maydis*. *Curr. Genet.* **53**, 49 (2008).
17. R. Montrocher, M. C. Verner, J. Briolay, C. Gautier, R. Marmeisse, Phylogenetic analysis of the *Saccharomyces cerevisiae* group based on polymorphisms of rDNA spacer sequences. *Int. J. Syst. Bacteriol.* **48**, 295 (1998).
18. G. C. Segers, X. Zhang, F. Deng, Q. Sun, D. L. Nuss, Evidence that RNA silencing functions as an antiviral defense mechanism in fungi. *Proc. Natl. Acad.*

Sci. U S A **104**, 12902 (2007).
19. M. J. Schmitt, F. Neuhausen, Killer toxin-secreting double-stranded RNA mycoviruses in the yeasts *Hanseniaspora uvarum* and *Zygosaccharomyces bailii*. *J. Virol.* **68**, 1765 (1994).
20. F. Radler, S. Herzberger, I. Schonig, P. Schwarz, Investigation of a killer strain of *Zygosaccharomyces bailii*. *J. Gen. Microbiol.* **139**, 495 (1993).
21. Y. Koltin, P. R. Day, Inheritance of killer phenotypes and double-stranded RNA in *Ustilago maydis*. *Proc. Natl. Acad. Sci. U S A* **73**, 594 (1976).
22. Y. Koltin, P. R. Day, Specificity of *Ustilago maydis* killer proteins. *Appl. Microbiol.* **30**, 694 (1975).
23. J. D. Thompson, D. G. Higgins, T. J. Gibson, CLUSTAL W: Improving the sensitivity of progressive multiple sequence alignment through sequence weighting, position-specific gap penalties and weight matrix choice. *Nucleic Acids Res.* **22**, 4673 (1994).
24. N. Romano, G. Macino, Quelling: Transient inactivation of gene expression in *Neurospora crassa* by transformation with homologous sequences. *Mol. Microbiol.* **6**, 3343 (1992).
25. P. K. Shiu, N. B. Raju, D. Zickler, R. L. Metzenberg, Meiotic silencing by unpaired DNA. *Cell* **107**, 905 (2001).
26. A. L. Goldstein, J. H. McCusker, Three new dominant drug resistance cassettes for gene disruption in *Saccharomyces cerevisiae*. *Yeast* **15**, 1541 (1999).
27. G. I. Naumov, S. A. James, E. S. Naumova, E. J. Louis, I. N. Roberts, Three new species in the *Saccharomyces* sensu stricto complex: *Saccharomyces cariocanus*, *Saccharomyces kudriavzevii* and *Saccharomyces mikatae*. *Int. J. Syst. Evol. Microbiol.* **50**, 1931 (2000).
28. F. Radler, M. J. Schmitt, B. Meyer, Killer toxin of *Hanseniaspora uvarum*. *Arch. Microbiol.* **154**, 175 (1990).
29. J. G. Menzies, G. Bakkeren, F. Matheson, J. D. Procunier, S. Woods, Use of inter-simple sequence repeats and amplified fragment length polymorphisms to analyze genetic relationships among small grain-infecting species of ustilago. *Phytopathology* **93**, 167 (2003).
30. G. Bakkeren, J. W. Kronstad, Conservation of the b mating-type gene complex among bipolar and tetrapolar smut fungi. *Plant Cell* **5**, 123 (1993).
31. M. J. McCullough, K. V. Clemons, J. H. McCusker, D. A. Stevens, Intergenic transcribed spacer PCR ribotyping for differentiation of *Saccharomyces* species and interspecific hybrids. *J. Clin. Microbiol.* **36**, 1035 (Apr, 1998).
32. M. Maiwald, R. Kappe, H. G. Sonntag, Rapid presumptive identification of medically relevant yeasts to the species level by polymerase chain reaction and restriction enzyme analysis. *J. Med. Vet. Mycol.* **32**, 115 (1994).
33. D. R. Scannell *et al.*, Independent sorting-out of thousands of duplicated gene pairs in two yeast species descended from a whole-genome duplication. *Proc. Natl. Acad. Sci. U S A* **104**, 8397 (2007).
34. M. Kellis, B. W. Birren, E. S. Lander, Proof and evolutionary analysis of ancient genome duplication in the yeast *Saccharomyces cerevisiae*. *Nature* **428**, 617 (2004).
35. P. Cliften *et al.*, Finding functional features in *Saccharomyces* genomes by

phylogenetic footprinting. *Science* **301**, 71 (2003); 10.1126/science.1084337.
36. A. R. Butler, J. H. White, M. J. Stark, Analysis of the response of *Saccharomyces cerevisiae* cells to *Kluyveromyces lactis* toxin. *J. Gen. Microbiol.* **137**, 1749 (1991).
37. R. F. Petersen *et al.*, Inheritance and organisation of the mitochondrial genome differ between two *Saccharomyces* yeasts. *J. Mol. Biol.* **318**, 627 (2002).
38. N. Cadez, P. Raspor, M. T. Smith, Phylogenetic placement of *Hanseniaspora-Kloeckera* species using multigene sequence analysis with taxonomic implications: Descriptions of *Hanseniaspora pseudoguilliermondii* sp. nov. and *Hanseniaspora occidentalis* var. *citrica* var. nov. *Int. J. Syst. Evol. Microbiol.* **56**, 1157 (2006).
39. Y. Ben-Yephet *et al*., Inheritance of Tolerance to Carboxin and Benomyl in *Ustilago hordei. Phytopathology* **65**, 563 (1975).
40. P. C. Thomas, thesis, University of Alberta, Edmonston, Canada (1965).
41. G. Bakkeren, J. W. Kronstad, C. A. Levesque, Comparison of AFLP Fingerprints and ITS Sequences as Phylogenetic Markers in Ustilaginomycetes. *Mycologia* **92,** 510 (2000).
42. R. B. Wickner, Double-stranded RNA viruses of *Saccharomyces cerevisiae*. *Microbiol. Rev.* **60**, 250 (1996).
43. F. Rodrigues *et al*., The spoilage yeast *Zygosaccharomyces bailii* forms mitotic spores: A screening method for haploidization. *Appl. Environ. Microbiol.* **69**, 649 (2003).
44. S. Kagiyama, T. Aiba, K. Kadowaki, K. Mogi, New killer toxins of halophilic *Hansenula anomala*. *Agric. Biol. Chem*. **52**, 1 (1988).
45. Y. Yamada, K. Mikata, I. Banno, Reidentification of 121 srains of the genus *Saccharomyces*. *Bull JFCC* **9**, 95 (1993).
46. R. B. Wickner, in *Viruses of Yeasts, Fungi and Parasitic Microorganisms*, vol. 1 of *Field's Virology*, B. N. Fields, D. M. Knipe, P. M. Howley Eds. (Raven, New York, ed. 5, 2001), pp. 629–658.

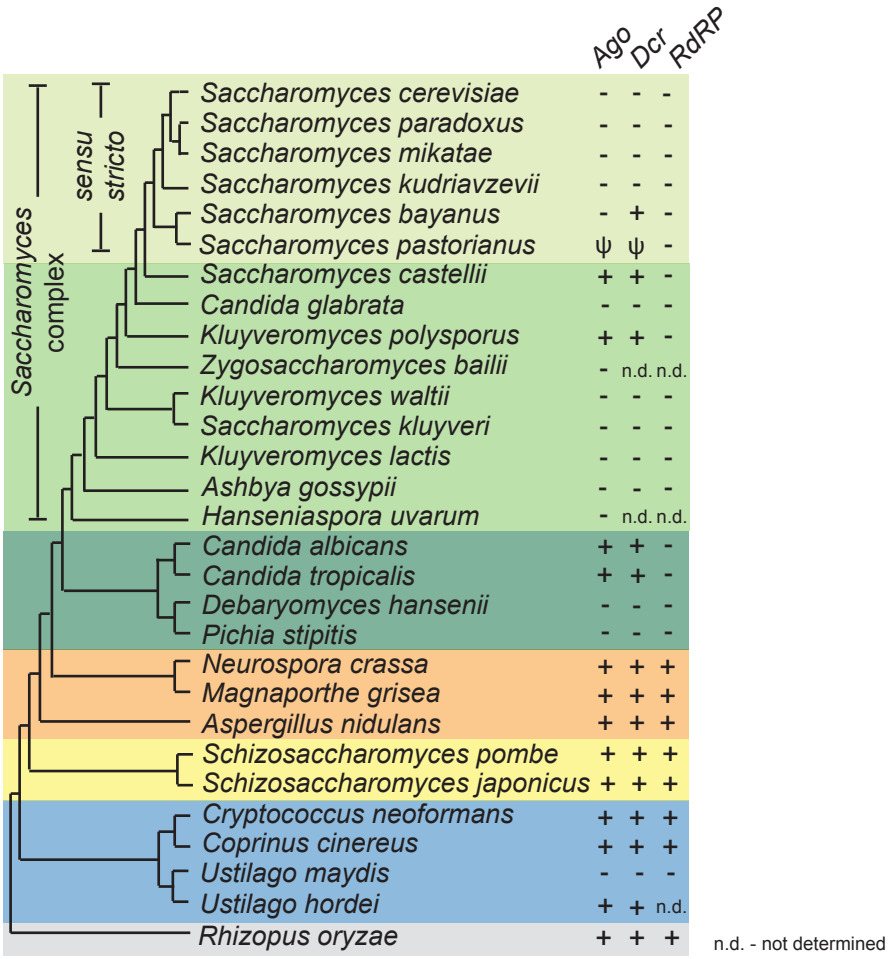

Figure S1. Cladogram showing Basidiomycota (blue), Zygomycota (grey) and Ascomycota, subdivided into Saccharomycotina (budding yeasts, light, medium and dark green), Pezizomycotina (orange) and Taphrinomycotina (yellow) (*13*, *14*). The presence of RNAi genes is indicated (+) (refs. *1, 15, 16* and references therein, and current study). Pseudogenes are indicated (Ψ). *Saccharomyces bayanus*, which has a Dicer but not an Argonaute gene, appears to lack siRNAs (*1*).

All sequenced species of the *sensu stricto* clade lack the RNAi pathway (defined as the presence of homologs for both Argonaute and Dicer). Therefore, the simplest model (and the one mentioned in the text) would be a loss of RNAi in a common ancestor of *sensu stricto* yeast species. Nevertheless, *Saccharomyces pastorianus*, a hybrid between *S. cerevisiae* and *S. bayanus* strains, still has pseudogenes for both Argonaute and Dicer, which have presumably been inherited from the genome of the *S. bayanus* strain (*17*). The short lifespan of pseudogenes in yeast genomes suggests that RNAi was lost in this lineage more recently than the *sensu stricto* radiation. Perhaps RNAi was lost twice, once in a common ancestor of *S. cerevisiae*, *Saccharomyces paradoxus*, *Saccharomyces mikatae* and *Saccharomyces kudriavzevii*, and once with the creation of an *AGO1* pseudogene in the *S. bayanus* lineage before the event that gave rise to *S. pastorianus*. In this scenario, loss of the *AGO1* pseudogene in *S. bayanus* and creation of the *DCR1* pseudogene in *S. pastorianus* would have followed the emergence of *S. pastorianus*. Another possibility is that RNAi was lost three times, once in a common ancestor of *S. cerevisiae*, *S. paradoxus*, *S. mikatae* and *S. kudriavzevii*, once in the *S. pastorianus* lineage, and once in the *S. bayanus* lineage. This scenario implies that some extant *sensu stricto* species closely related to the sequenced *S. pastorianus* and *S. bayanus* strains might still retain an active RNAi pathway.

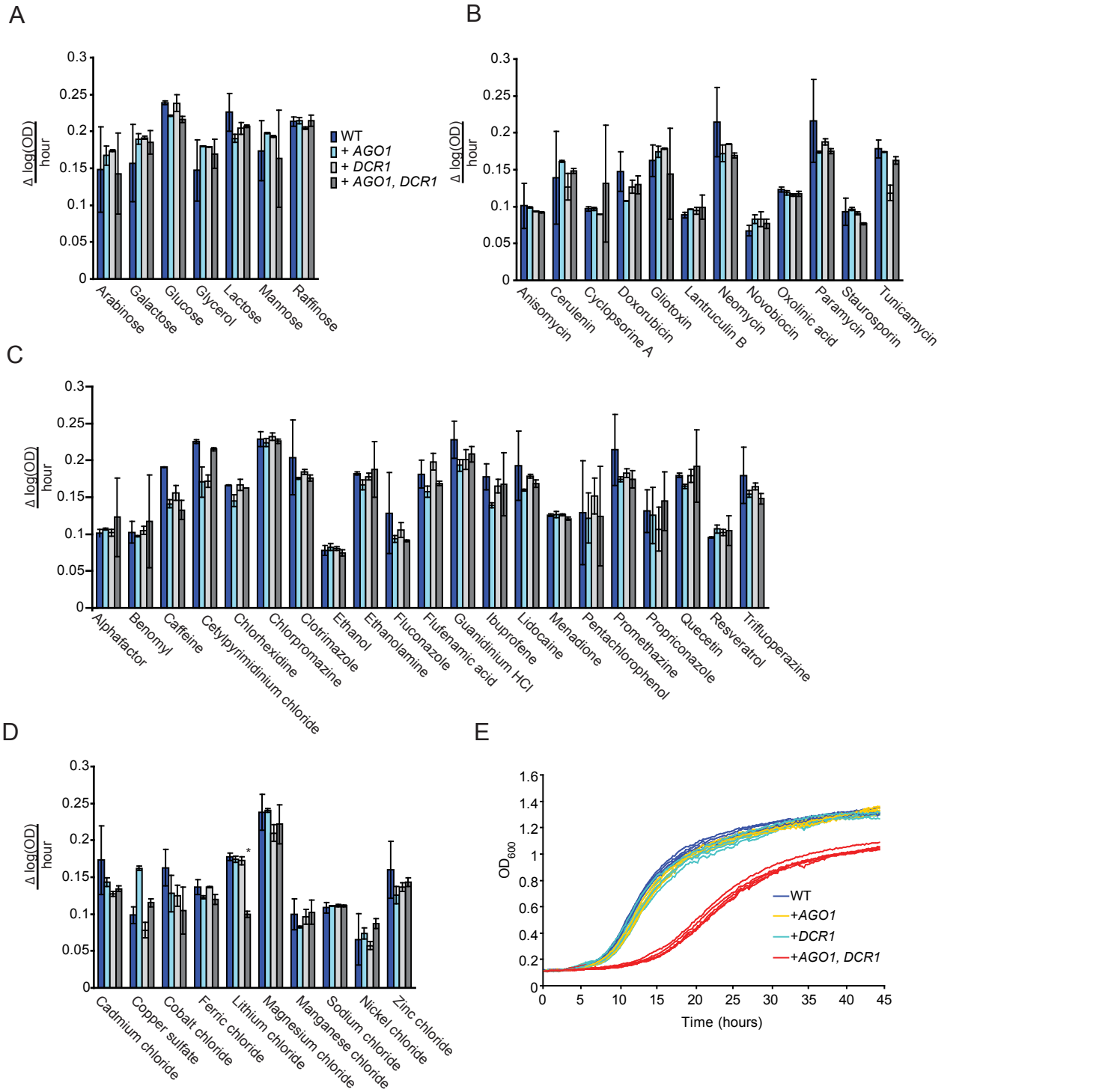

Figure S2. Phenotypic profiling of *S. cerevisiae* wild-type (WT), +*AGO1*, +*DCR1* and +*AGO1*, *DCR1* strains in 50 different conditions (table S5). (**A–D**) Two replicates of WT (DPB249), +*AGO1* (DPB252), +*DCR1* (DPB255) and +*AGO1*, *DCR1* (DPB258) strains were grown in complete synthetic media at 30°C in the presence of the indicated carbon sources (**A**), antibiotics (**B**), other compounds, including fungicides (**C**), or salts (**D**), and the OD_{600} was measured every 15 minutes using the Bioscreen platform (Growth Curves USA). Plotted is the maximum slope of the linear part of each growth curve, calculated after log-transforming the OD_{600} values (bar, average of the two values; error bars, range). For one condition (200 mM LiCl), the two values from the RNAi-reconstituted strain fell outside the range of the six values from the other three strains (*). (**E**) Confirmation of the growth difference in 200 mM LiCl. Shown are growth curves for five replicates of each strain (P = 0.0012, Wilcoxon Rank Sum Test).

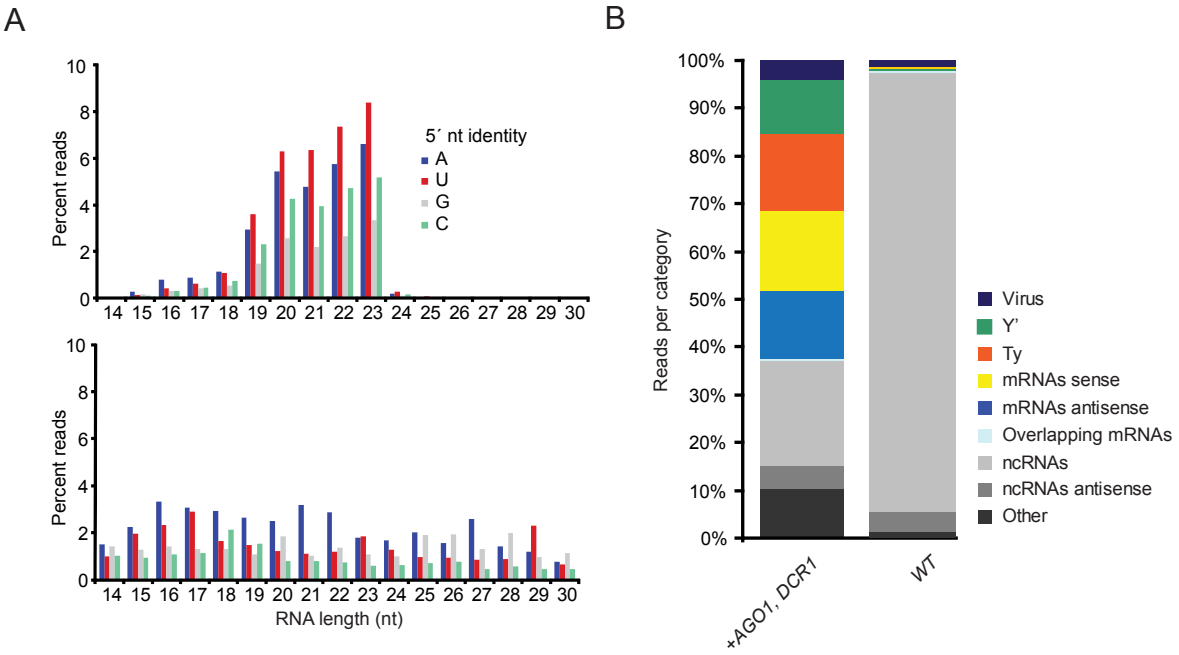

Figure S3. The small RNAs in *S. cerevisiae* with and without the RNAi pathway. (**A**) High-throughput sequencing of small RNAs in the RNAi-reconstituted *S. cerevisiae* (+*AGO1*, *DCR1*; top) and the parental strain (WT; bottom). Genome-matching sequencing reads representing small RNAs with the indicated length and 5' nucleotide are plotted as percent of total genome-matching reads. (**B**) Annotations of genomic loci (key) matching small RNA reads (table S1). 22–23-nt reads from the indicated strains are considered.

As in *S. castellii* (*1*), which naturally has RNAi, the most abundant small RNAs in the reconstituted *S. cerevisiae* strain were 23-nt RNAs that began with a U, and as expected of siRNAs, these small RNAs required the *S. castellii AGO1* and *DCR1* genes for their production and accumulation (panel A). However, length and 5' nt biases of the siRNAs sequenced from the RNAi-reconstituted *S. cerevisiae* strain were not as strong as those of the *S. castellii* siRNAs (*1*). The weaker length bias was consistent with RNA-blot results probing for small RNAs derived from Ty1 elements in *S. cerevisiae* expressing both *AGO1* and *DCR1* (*1*). Interestingly, the weaker length bias observed in the RNA blot seems dependent on *AGO1* because the shorter products were much less prominent in the sample from *S. cerevisiae* expressing *DCR1* alone (*1*).

Consistent with RNAi-mediated silencing of endogenous Ty1 elements observed in the reconstituted strain (*1*), about 17% of the siRNAs mapped to Ty elements (panel B), preferentially of the Ty1 and Ty2 classes (fig. S4). Another large fraction of the siRNAs (12%) mapped to Y' elements, which are non-transposon repeats that reside near telomeres and encode a large conserved protein with a helicase domain. About a third of the siRNAs mapped to open reading frames (ORFs), either in the sense or antisense orientation. This fraction of ORF-derived siRNAs was almost threefold greater in *S. cerevisiae* compared to *S. castellii* (table S1). Despite the greater fraction of mRNA-derived siRNAs, our strand-specific mRNA-Seq results showed that *S. cerevisiae* and *S. castellii* had comparable antisense transcription of ORFs (table S2). Perhaps the absolute number of siRNAs mapping to non-repetitive ORFs was not greater in *S. cerevisiae*, and the greater fraction is explained by relatively few siRNAs deriving from non-coding transcripts, whereas in *S. castellii* large amounts of dsRNA produced from repetitive and non-coding transcripts (e.g., hairpin transcripts homologous to transposon fragments) contribute a large fraction of its siRNAs. Alternatively, the absolute number of siRNAs mapping to non-repetitive ORFs might have been greater in *S. cerevisiae*, perhaps a result of the RNAi machinery not being titrated by an abundance of non-coding dsRNA.

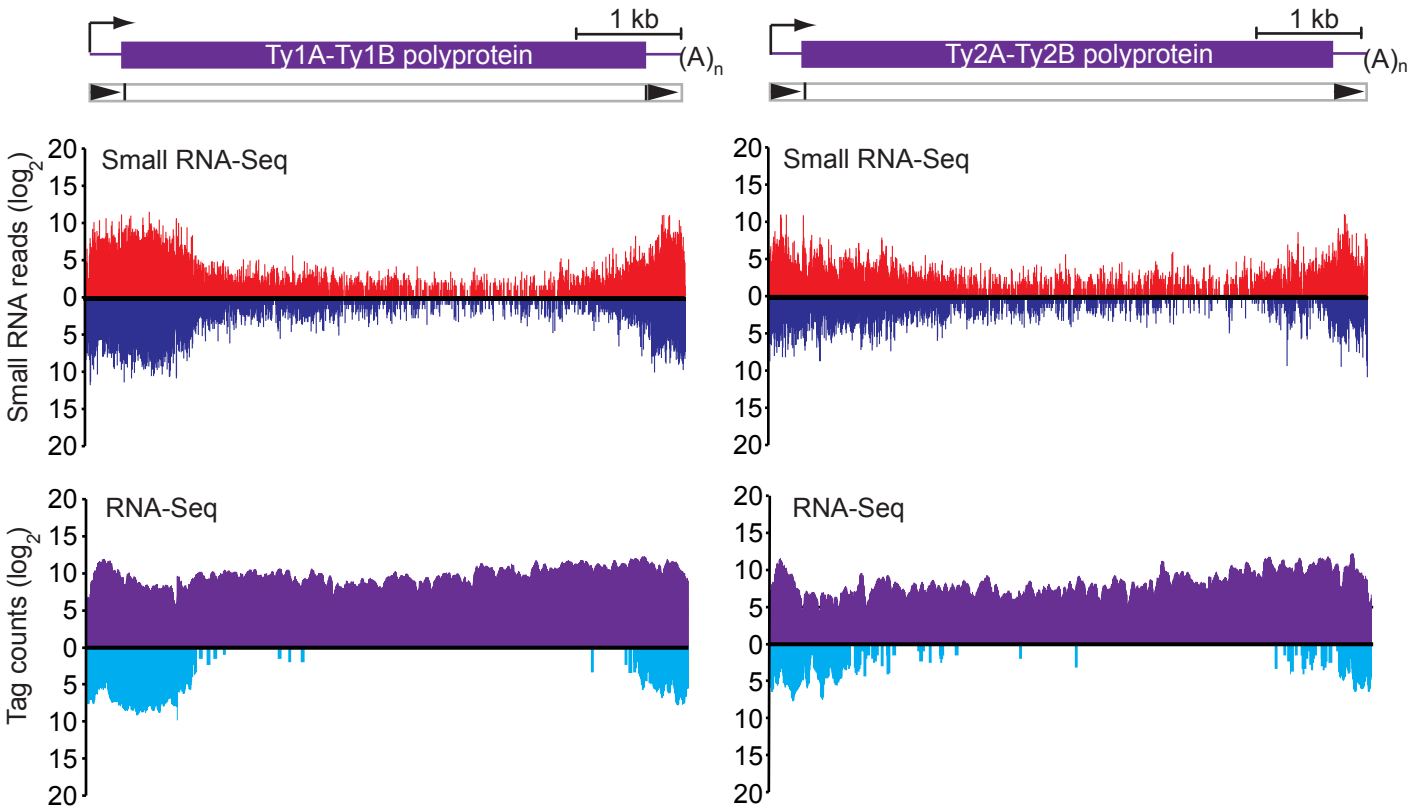

Figure S4. Small RNAs and transcripts mapping to *S. cerevisiae* Ty1 and Ty2 elements. The schematic shows Ty1 and Ty2 transcripts (purple) and elements (black), with long terminal repeats as black triangles. The numbers of small-RNA 5' ends (middle) and RNA-Seq tags (bottom) mapping to a consensus Ty1 (left) and Ty2 (right) element are plotted for each position (sense, above axis; antisense, below axis). All full-length Ty1 or Ty2 elements in the S288C genome sequence were aligned using SeqMan Pro (DNASTAR Lasergene). Small-RNA reads (22–23-nt sequences) from the RNAi-reconstituted *S. cerevisiae* strain and RNA-Seq tags from the *S. cerevisiae* wild-type were initially mapped to the set of individual Ty1 or Ty2 elements, allowing no mismatches and normalizing by the number of hits to the elements. Mapped nucleotide positions with respect to individual elements were then converted into positions with respect to the consensus.

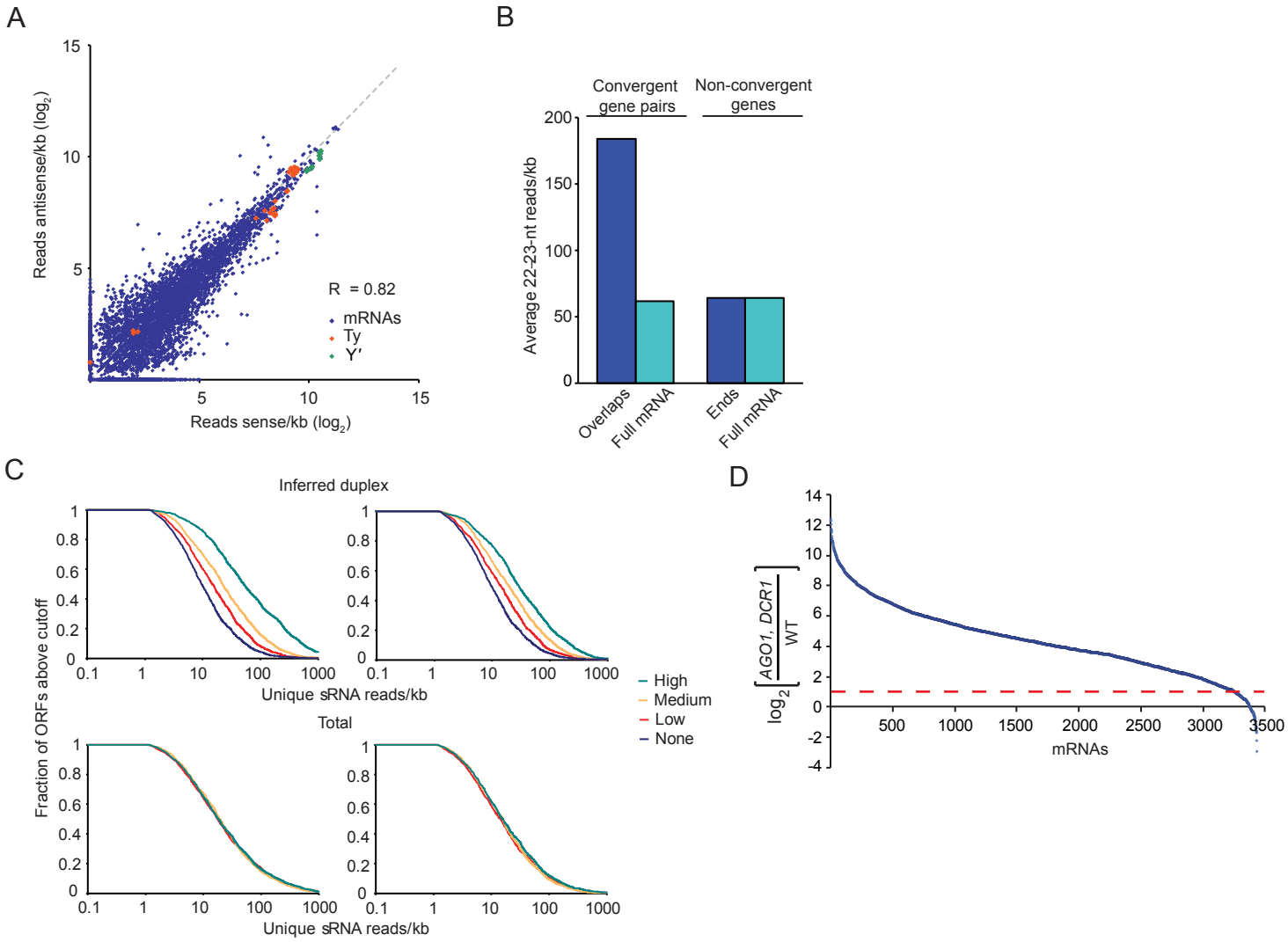

Figure S5. Correlation between siRNA reads and inferred dsRNA. (**A**) Strand orientation of small RNAs mapping to mRNAs. Results for mRNAs of the Ty and Y' repeats are indicated separately (key). (**B**) Evidence for siRNAs deriving from overlapping regions of convergent mRNAs. A gene pair was defined as a protein-coding gene and its closest right neighbor (according to YGOB annotations). Out of 1231 convergent gene pairs, 778 overlapped at their 3' ends. Read densities of 22–23-nt sequences for overlapping regions longer than 23 nt (712 overlaps) were calculated and compared to read densities of their convergent full-length mRNAs (bars on left). The median overlap was 169 nt. As a control, read densities of 22–23-nt sequences were calculated in the 3' terminal 169 nt of non-convergent genes and compared to read densities of the full-length mRNAs (bars on right). (**C**) Correlation between transcript abundance and small-RNA density for annotated ORFs. ORFs were binned according to inferred-duplex abundance (estimated as the abundance of the limiting strand; left top) or total transcript abundance (sum of sense and antisense tags, left bottom). ORFs with zero inferred-duplex abundance (i.e., ORFs with sense tags but no antisense tags) formed a fourth bin (none). Plotted is the fraction of ORFs within a given bin that has at least as many uniquely matching small RNA reads (on either strand) as the *x* axis value. As expected if siRNAs in coding sequences derived from dsRNA precursors formed by sense-antisense transcript pairs, the abundance of ORF siRNAs correlated with the abundance of the inferred duplex [$P = 10^{-16}$, $P = 10^{-15}$, $P = 10^{-14}$ for comparing no-duplex (blue) to low (red), low to medium (yellow) and medium to high (green), respectively, Kolmogorov-Smirnov test], whereas the abundance of ORF siRNAs did not correlate with the total abundance of sense and antisense transcripts [$P = 0.25$, $P = 0.80$ and $P = 0.12$ for comparing low (red) to medium (yellow), medium to high (green) and low to high, respectively]. After removing all convergent overlapping gene pairs that gave rise to small RNAs in the overlap region (right top, right bottom), the correlation of siRNAs with inferred duplex was still significant [$P = 10^{-16}$, $P = 10^{-12}$, $P = 10^{-12}$ for comparing no duplex (blue) to low (red), low to medium (yellow) and medium to high (green), respectively], in contrast to a weaker but significant correlation with total sense and antisense transcript abundance [$P = 0.35$, $P = 0.01$ and $P = 10^{-3}$ for comparing low to medium (yellow) and medium to high (green), and low to high respectively, Kolmogorov-Smirnov test]. For each ORF, matching RNA-Seq tags and small-RNA reads were identified, considering only those that mapped to a single genomic locus. ORFs with no unique RNA-Seq tags mapping to the coding strand and those with less than a twofold increase of 22–23-nt small-RNA reads in the sequencing run from the

Continue Figure S5.
RNAi-reconstituted *S. cerevisiae* strain compared to the wild-type strain were excluded. (**D**) RNAi dependence of siRNAs from mRNAs. Small RNAs sequenced in the RNAi-reconstituted strain (*AGO1*, *DCR1*) and parental strain (WT) were mapped to mRNAs, considering both sense an antisense orientations. For the 3438 mRNAs with at least 10 siRNA reads, the fold change in the reconstituted strain (after normalizing to the total number of genome-matching reads and adding a pseudocount of 1 to both values) was calculated, ranked and plotted. Among the 3438 mRNAs, 3252 had at least twofold more siRNA reads in the sample from the RNAi-reconstituted strain (above dashed red line).

Three lines of evidence indicated that the siRNAs that matched mRNAs were produced from dsRNA: 1) a correlation between the abundance of sense siRNAs and antisense siRNAs from each mRNA locus (panel A), 2) an enrichment of siRNAs in regions where convergent mRNAs overlap (panel B), and 3) a strong correlation between siRNA abundance and the amount of the inferred duplex, as estimated by the least abundant transcript of each sense-antisense transcript pair (panel C). With these in mind, our results showed that mRNAs from more than 3200 *S. cerevisiae* genes form dsRNA in vivo (panel D).

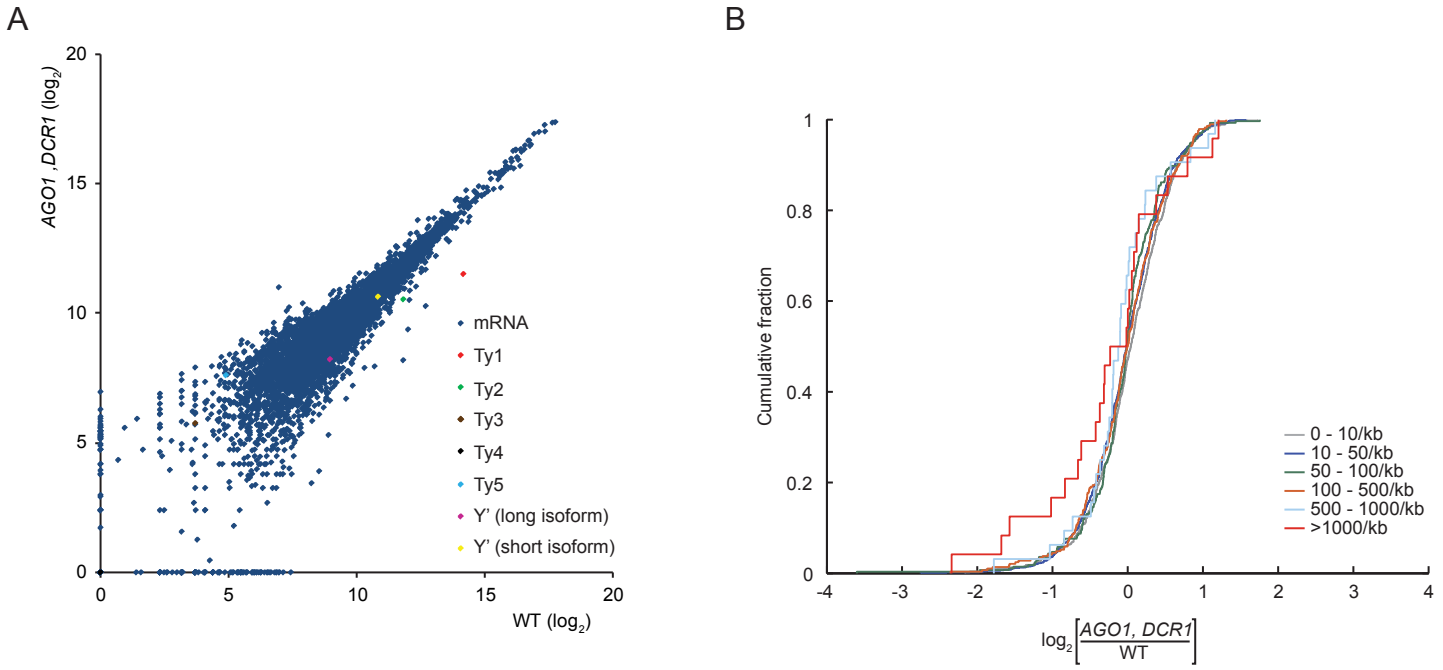

Figure S6. The effect of RNAi on endogenous gene expression in *S. cerevisiae*. (**A**) mRNA expression changes in the RNAi-reconstituted strain, as measured by RNA-Seq. Plotted are the $\log_2$ ratios of RNA-Seq tags per kb in wild-type (*x* axis) versus the RNAi-reconstituted strain (*y* axis) (after adding a pseudocount of 1 to both values). To measure mRNA abundance from non-repetitive genes only uniquely mapping RNA-Seq tags were considered. Transcript abundance of Ty1-4 (Ty5 has only a single copy in the *S. cerevisiae* genome) and the short and long isoforms of Y' elements were estimated after mapping RNA-Seq tags to their consensus elements. Because RNA-Seq was performed on poly(A)-selected RNA, tags were generated from 3' degradation fragments of RNAi-targeted transcripts (*1*). To better measure abundance of full-length transcripts, only tags mapping to 5'-most 250 nt of each transcript were considered (excluding the 5' LTRs of Ty elements, because tags mapping to these regions might have derived from the 3' LTRs). Nonetheless, the change in abundance of full-length Ty1 mRNA measured by RNA-blotting is more substantial (*1*). The marginal down-regulation of Y' mRNA in the RNAi-reconstituted strain compared to the wild-type strain contrasted to the substantial reduction of Y' mRNA in the RNAi-reconstituted strain compared to the strain expressing only Ago1 (table S2). In the presence of Ago1, Y' mRNAs increased 5 fold compared to the wild-type strain. In addition, the strain expressing only Ago1 had increased antisense transcripts to ORFs (2.2 fold), increased Ty transcripts, especially those mapping in the antisense orientation (2 fold), and increased killer satellite–derived mRNA (2.5 fold) (table S2). The increased accumulation of killer satellite–derived mRNA was consistent with the observation that none of the Ago1-expressing colonies lost the killer satellite dsRNA (Fig. 1A). Perhaps Ago1 binds and inhibits RNA-degradation enzymes, and this explains the effects of expressing only Ago1 in *S. cerevisiae*, but this hypothesis has not been tested. (**B**) Effect of RNAi on expression of genes that are not repetitive elements. Changes in mRNA levels after introduction of RNAi were determined as in panel A, and groups of mRNAs were binned according to their small-RNA read density (per kb). Plotted for each bin is the fraction of mRNAs that change at least to the degree indicated on the *x* axis. Only mRNAs with more than twofold increased 22–23-nt small-RNA reads in the RNAi-reconstituted strain compared to the wild-type and those with more than 100 reads in the wild-type RNA-Seq library were considered in this analysis. The distributions of changes were not significant for most pair-wise comparisons, except for a marginal significance observed between 0–10/kb (grey) and 50–100/kb (green) ($P = 0.01$ Kolmogorov–Smirnov test). As in *S. castellii* (*1*) the RNAi pathway in *S. cerevisiae* had little, if any, impact on accumulation of nonrepetitive mRNAs, which is consistent with the near absence of phenotypic effects (fig. S2). This subtle and benign impact of RNAi on molecular and cellular phenotype bodes well for its utility as a research tool in *S. cerevisiae*, as it can be utilized without major side effects.

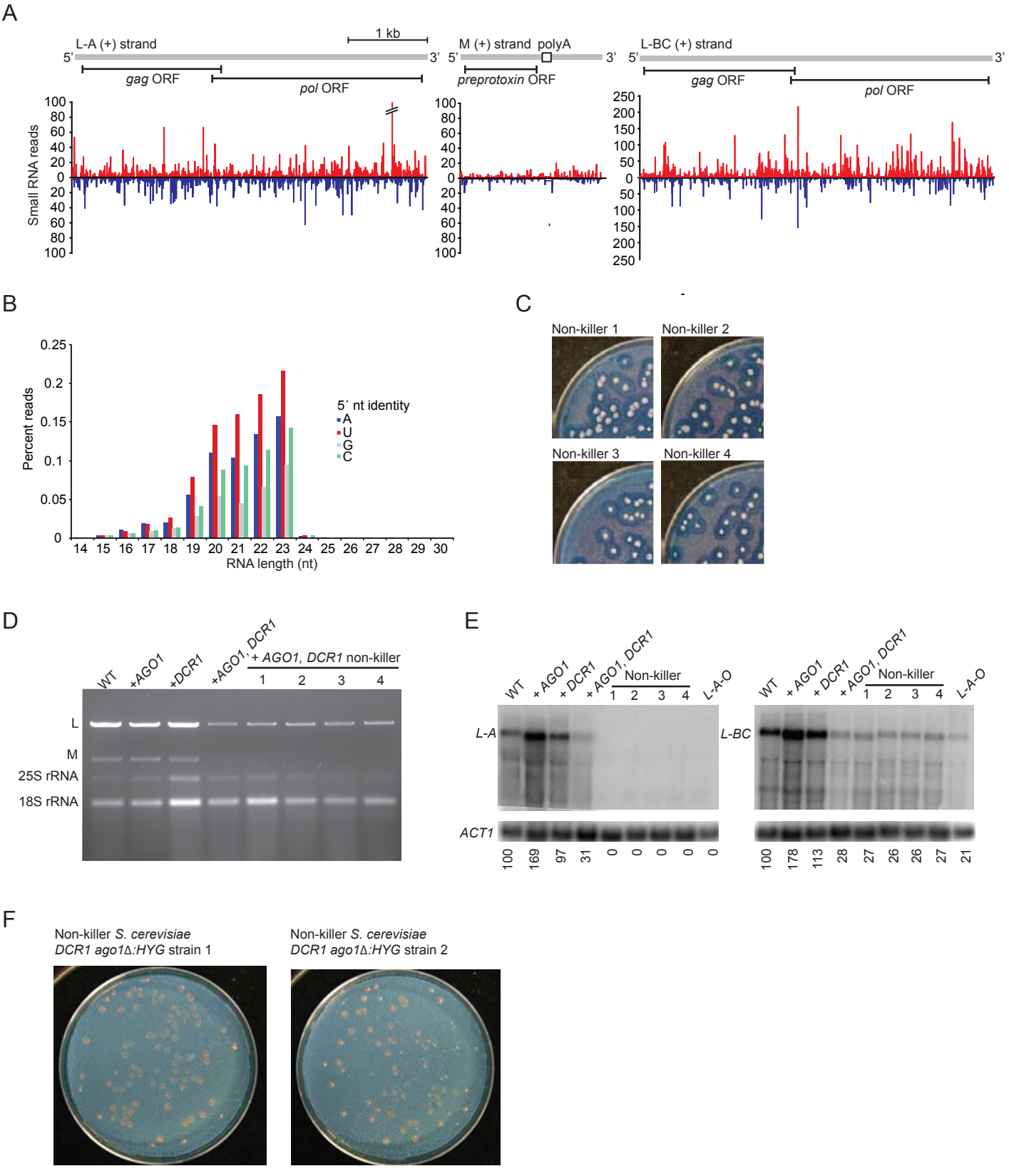

Figure S7. RNAi targeting of the endogenous killer virus of *S. cerevisiae.* (**A**) siRNAs mapping to dsRNA genome of L-A, M, and L-BC. The numbers of small RNA 5' ends (22–23-nt sequences) are plotted for each position across the genomes (sense, above axis; antisense, below axis). The higher levels of L-BC siRNAs presumably reflected the fact that most cells have lost L-A and M. (**B**) Profile of the sequenced small RNAs mapping to L-A, L-BC and M genomes from the RNAi-reconstituted *S. cerevisiae* strain. Otherwise, as in figure S3A. (**C**) Sensitivity of isolates that lost killer activity. Four isolates of the RNAi-reconstituted strain that had each lost killer activity in the killer plate assay were plated as a lawn and

Continue Figure S7.
for sensitivity to the toxin secreted by colonies of the parental wild-type strain. (**D**) Loss of M dsRNA in isolates that lost killer activity. dsRNA purified from the indicated *S. cerevisiae* strains and four non-killer isolates identified by the killer plate assay was fractionated on agarose-gels and stained with ethidium bromide. (**E**) Loss of L-A dsRNA in isolates that lost killer activity. mRNA derived from the strains of Figure 1A and *L-A-O*, a strain known to lack L-A (*7*), were analyzed using RNA blots. The blots were probed for either *L-A* (left) or *L-BC* (right) transcripts and then were probed for *ACT1*, which was used to normalize for loading when quantifying the relative levels of viral transcripts (bottom). Consistent with RNA-Seq data (table S2), *L-BC* and *L-A* transcripts were up-regulated in the strain expressing only Ago1. (**F**) Irreversible loss of killer in the RNAi-reconstituted strain. *AGO1* was deleted in cells from two colonies (isolate 1 and 2) that had lost their ability to kill the sensitive strain (Fig. 1A), and killing capacity of these cells in which the RNAi pathway had been disrupted was monitored using the killer plate assay. No recovery of the killer phenotype was observed, which ruled out persistent infection by killer at low levels, thereby implying a complete loss of the killer element. The integrated *S. castellii AGO1* was deleted by homologous recombination, using the hygromycin cassette of pAG32 (*26*) amplified with the following primers:
5´CTACTGAAGGTGCCACAGAAGATAAACCTAAGAAGGTTAAGCCCTACCCGGCGCCAGATCTGTTTAGCTT
5´GACAACACAAATTGTGGTGACAGATGGGTTATAGTTGACACCCTTGTTTAACTATAGGGAGACCGGCAGA.

Two cytoplasmatically inherited dsRNA viruses of the *Totiviridae* family, L-A and L-BC, are endemic to *S. cerevisiae* (*46*). Many strains that contain L-A also carry a dsRNA satellite of L-A, called M, which encodes a secreted protein toxin (the killer toxin) and imparts immunity to that toxin (*3*). The M dsRNA is dependent on its helper virus L-A for replication and encapsiculation. Together, L-A and M comprise the dsRNA killer system, because strains carrying both will kill strains lacking M.

We found that more than 2% of the siRNA reads mapped sense and antisense across the length of the three dsRNA genomes present in the parental *S. cerevisiae* strain (panel A), with length and 5'-nucleotide distributions indistinguishable from those of siRNAs from genomic loci (panel B). These killer siRNAs correlated with the loss of killing capacity for more than 90% of the cells soon after establishing the RNAi-reconstituted strain (Fig. 1A). Of the cells that retained killing capacity, most lost it after another round of overnight growth at 30°C in YPD liquid culture (data not shown). As expected, isolates that lost killer were susceptible to the toxin secreted by the parental strain (panel C). Cells that lost killing capacity also lost both the toxin-encoding satellite dsRNA M and its helper virus L-A (panels D and E). S dsRNAs, which are M deletion variants that can displace M by virtue of their faster replication (*8*), were not detected in any of the isolates that lost killing capacity. Although reduced in abundance, the L-BC genome was retained (panel E). Perhaps L-BC is under stronger or more continuous selection than are either M or L-A. In this scenario, dsRNA viruses that are under strong continuous selection can be retained in the presence of RNAi, which is consistent with the observation that some dsRNA viruses can persist in other RNAi-competent species (*18*). Killing capacity did not recover after *AGO1* was deleted, which indicated that the killer phenotype was irreversibly lost and not just repressed (panel F).

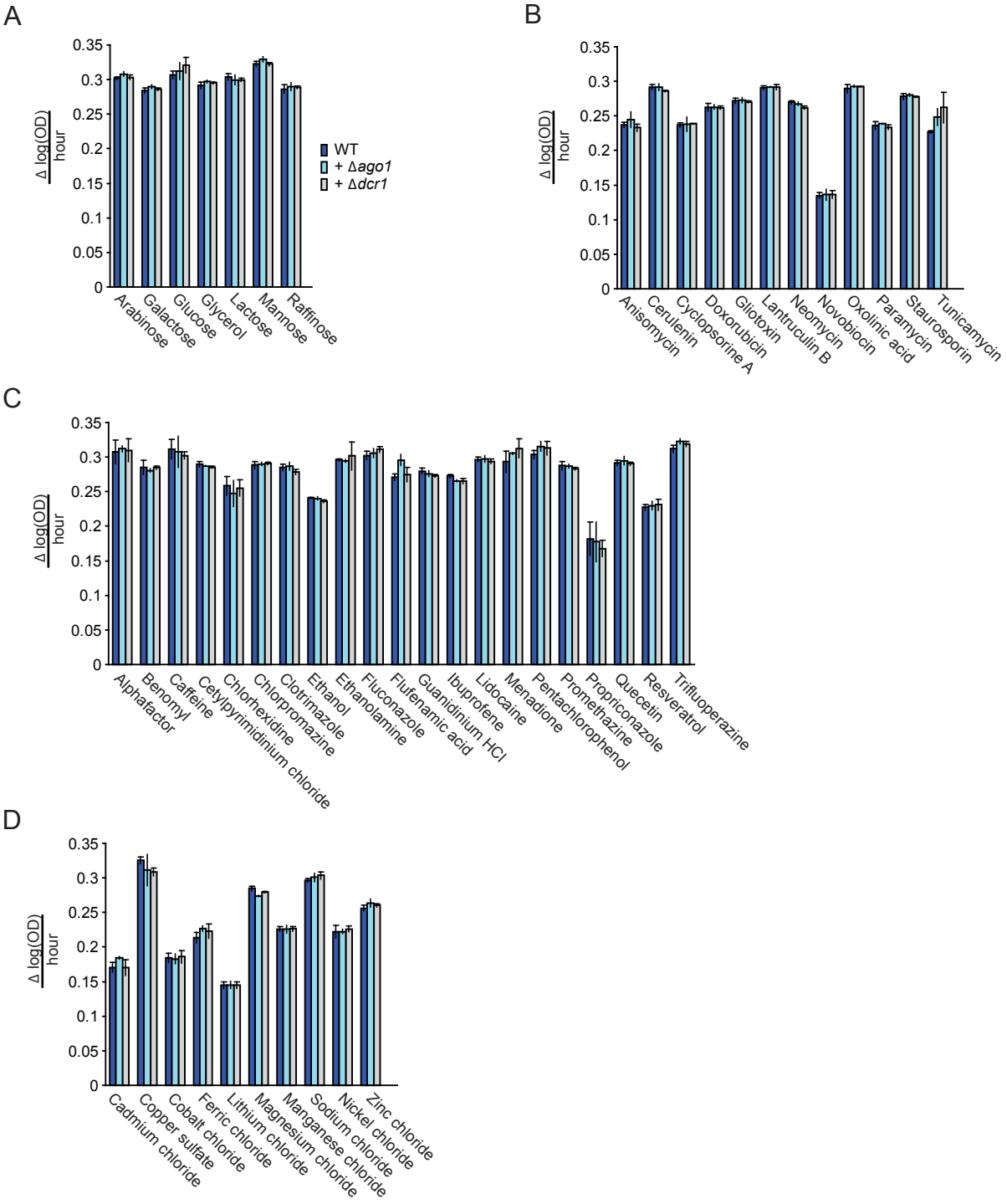

Figure S8. Phenotypic profiling of *S. castellii* WT, Δ*ago1* and Δ*dcr1* strains in 50 different conditions (table S5). (**A-D**) Three replicates of WT (DPB005), Δ*ago1* (DPB007), and Δ*dcr1* (DPB009) were grown in complete synthetic media at 25°C, otherwise as in figure S2. In each condition tested there was no significant growth difference between the three strains.

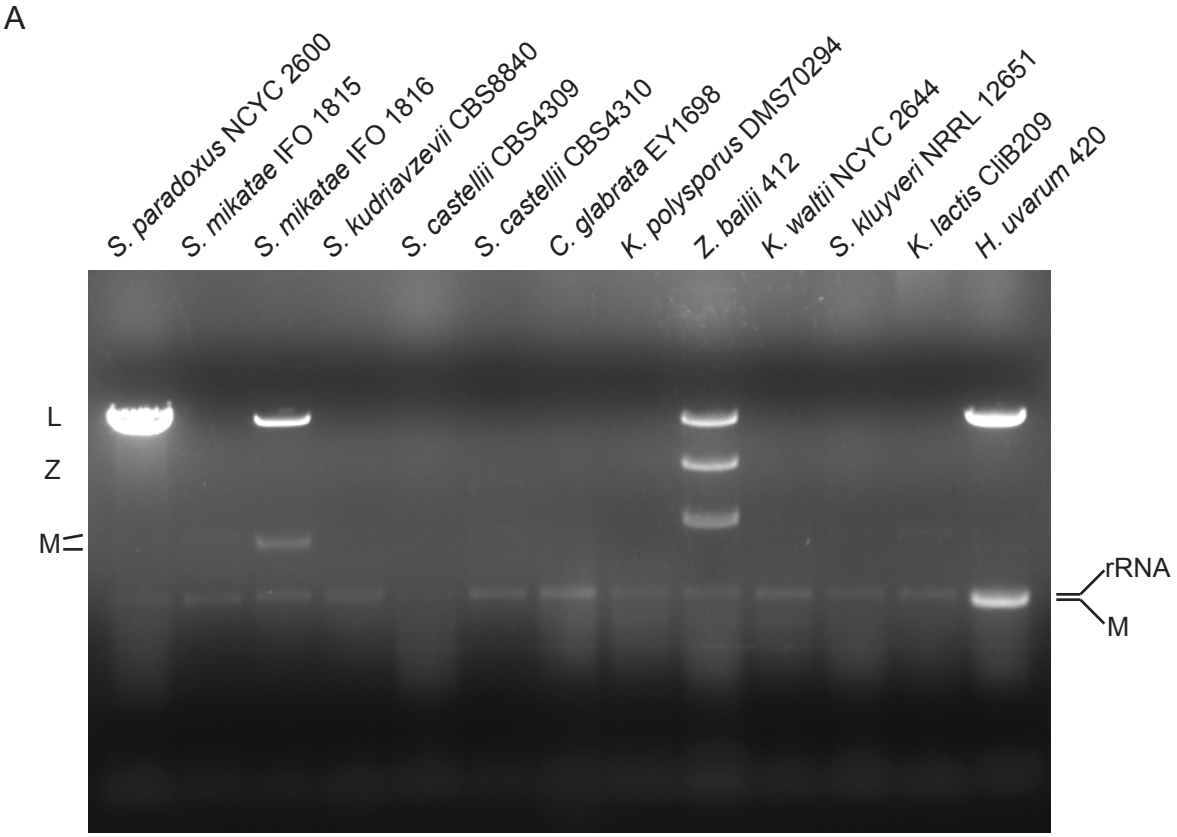

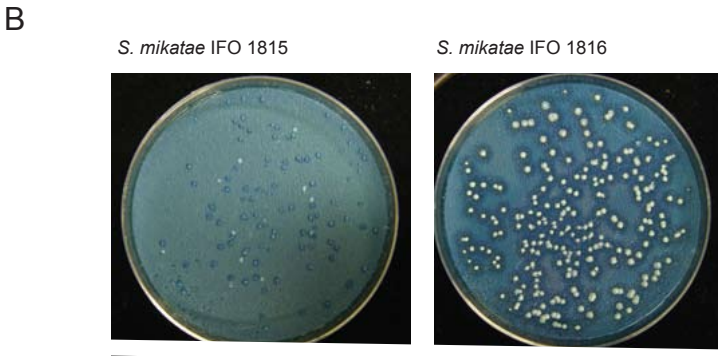

Figure S9. dsRNA killer viruses in budding yeasts. (**A**) dsRNA of the indicated budding-yeast species and strains, resolved on an agarose gel and visualized by ethidium-bromide staining. In addition to the L and M dsRNA genomes, *Zygosaccharomyces bailii* has a third dsRNA element, *Z*, which is thought to confer killer toxin immunity (*19*). (**B**) Killer plate assay of two different *S. mikatae* strains. The *S. cerevisiae L-A-O* strain was plated as the sensitive strain. Strain IFO 1816 exhibited the killer phenotype, consistent with its dsRNA pattern (panel A).

Close *S. cerevisiae* relatives belonging to the *sensu stricto* clade, including strains of *S. bayanus* (*6*), *S. paradoxus* (*5*) and *S. mikatae* (panel A), also have dsRNA killer viruses, and all sequenced species of the *sensu stricto* clade lack the RNAi pathway (defined as the presence of homologues for both Argonaute and Dicer) (fig. S1). In our model, the ability to acquire and maintain the killer system explains the success of this RNAi-deficient lineage. With regard to yeast species outside of the *sensu stricto* clade, our model predicted that no dsRNA killer viruses would be detected in the RNAi-positive yeast species, *S. castellii* and *Kluyveromyces polysporus*, which was indeed what we found (panel A). Considered together with the absence of RNAi in *Z. bailii* and *Hanseniaspora uvarum* (tables S3 and S4), which have dsRNA killer viruses (panel A) (*19*) the lack of killer in *S. castellii* and *K. polysporus* supported our conclusion that RNAi and dsRNA killer are incompatible, thereby extending our model for the success of RNAi-deficient species to events that occurred outside the *sensu stricto* clade of ascomycetous fungi (Fig. 1B).

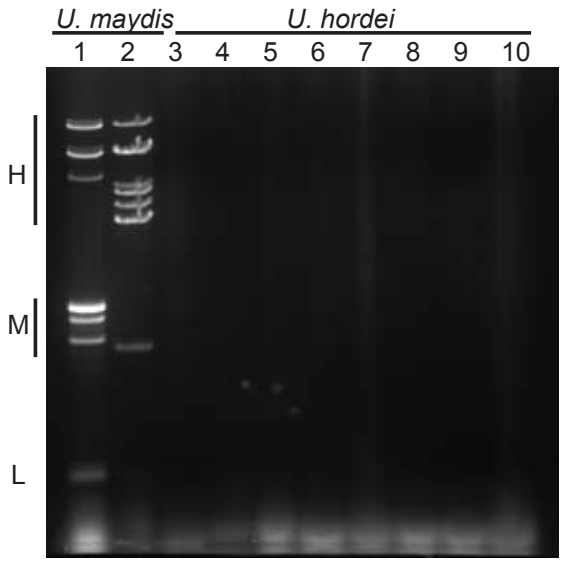

Figure S10. Absence of dsRNA viruses in *Ustilago hordei* isolates. dsRNA from two *Ustilago maydis* isolates [75 (44-2), 75 (45-2), lanes 1 and 2, respectively] and eight *U. hordei* isolates (car-4, I4, U807, Uh364, U809, Uh112, Uh362, Uh100, lanes 3–10) was fractionated on agarose-gels and stained with ethidium bromide.

Apart from the budding yeasts, dsRNA killer viruses have been found only in the maize smut fungus *U. maydis*, an evolutionarily distant basidiomycete (*21*). This was the only fungus outside of budding yeasts known to lack RNAi, but its close relative, *U. hordei*, has a functional RNAi pathway (*16*). To search for dsRNA killer viruses able to persist in the presence of RNAi, we looked for dsRNA elements in eight independent *U. hordei* isolates, including the Uh364 strain, which is known to be RNAi competent. None of the isolates contained any dsRNA elements, whereas dsRNAs corresponding to both the toxin-encoding satellite and the viral genomes were detected in two *U. maydis* strains included as controls. This result extended a previous study in which all of 16 tested *U. hordei* strains were sensitive to the *U. maydis* toxin, suggesting the absence of a related killer system in those strains (*22*).

A

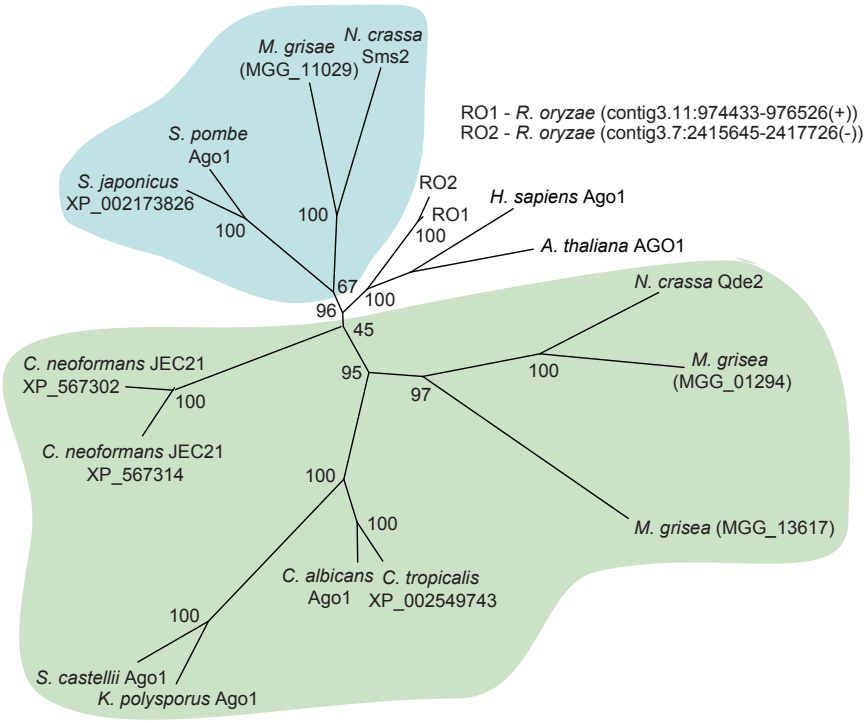

B

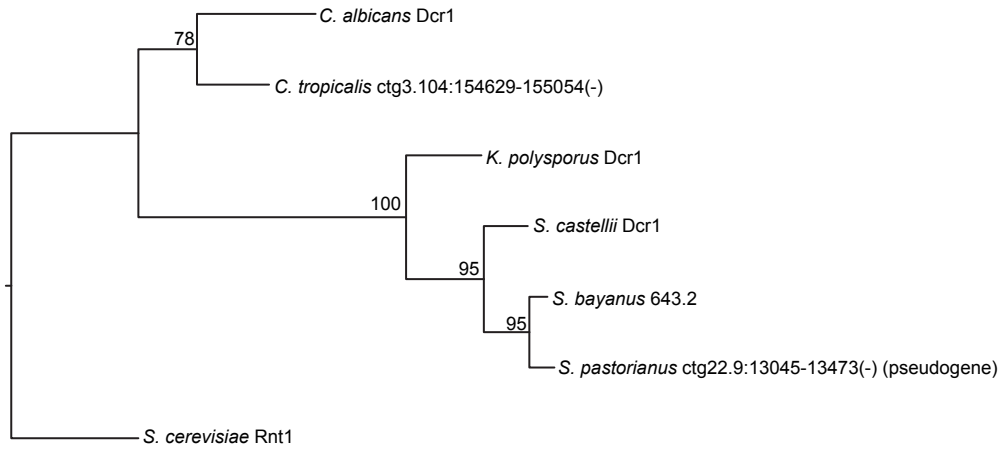

Figure S11. Evolution of fungal RNAi proteins. (**A**) Maximum-likelihood tree based on amino acid alignment of the indicated Argonaute proteins. The amino-acid sequences of the proteins (identified by gene names or accession numbers) were used to compute a multiple sequence alignment using the ClustalW software (*23*). A consensus ML tree was built by running PROML (PHYLIP http://evolution.genetics.washington.edu/phylip.html) on the amino acid alignment after bootstrap re-sampling (1000 replicates) of the data set using SEQBOOT (PHYLIP). The tree was displayed using TreeView (http://taxonomy.zoology.gla.ac.uk/rod/treeview.html). Bootstrap values are shown at nodes. The Arabidopsis *AGO1* was set as the outgroup. (**B**) Maximum-likelihood tree based on amino acid alignment of the RNase III domains of the indicated Dicer proteins. RNaseIII domain of *S. cerevisiae* Rnt1 was used as an outgroup because the budding-yeast Dicer probably emerged from a *RNT1* duplication early in the budding-yeast lineage (*1*). The budding-yeast Dicer topology was consistent with that of the background genomes. Alignment and tree construction were as in (A).

Consistent with previous analyses, ascomycete/basidiomycete Argonautes can be classified into two clades, implying that the common ancestor of ascomycetes and basidiomycetes had two Argonaute homologs (*15*). The topology of each Argonaute clade was consistent with that of the background genomes. Some species, including *N. crassa* and *M. grisae*, maintained at least one member of each clade. The common ancestor of the budding yeasts appears to have had only one of the two Argonaute homologs, the *N. crassa* Qde2 homolog, which is involved in the quelling pathway (*24*). A loss of the *N. crassa* Sms-2 homolog, which is involved in the meiotic silencing of unpaired DNA (MSUD) pathway (*25*), also occurred in the lineage of *C. neoformans*, whereas *S. pombe* and *S. japonicus* have lost the Qde2 homolog.

Table S1. Small-RNA sequencing data (22–23-nt reads) from *S. cerevisiae* wild-type and +*AGO1, DCR1* strains in comparison to the published small-RNA sequencing data from wild-type *S. castellii* (*1*). Numbers in parenthesis are percent of total genome-matching reads.
In the reconstituted strain, fewer reads corresponded to M and L-A RNAs than to L-BC RNA, as expected because both M and L-A were lost in most of the cells that had the RNAi pathway, whereas L-BC was reduced but not lost in these cells (fig. S7). Although the total number of small RNA reads mapping to M increased only slightly in the library of the RNAi-reconstituted strain, most small RNAs mapping to M in the RNAi-reconstituted strain exhibited features characteristic of siRNAs, whereas the small RNAs mapping to the M in the wild-type strain lacked the features characteristic of siRNAs but instead had features expected of RNA-degradation fragments.

	***S. castellii* wild-type**		***S. cerevisiae* +*AGO1, DCR1***		***S. cerevisiae* wild-type**	
Total genome-matching reads	400354.00	(100.00)	2108832.00	(100.00)	1525895.00	(100.00)
Non-ncRNA-matching reads *	325857.60	(81.39)	1627579.08	(77.18)	54956.65	(3.60)
L-A	–	–	13401.00	(0.64)	1086.00	(0.07)
L-BC	–	–	28871.00	(1.37)	882.00	(0.06)
M	–	–	1657.57	(0.08)	1486.03	(0.10)
Ty retrotransposons	91296.00	(22.80)	365373.21	(17.33)	3847.43	(0.25)
Y' elements	21947.70	(5.48)	254312.43	(12.06)	69.93	(<0.01)
mRNAs (sense)**	35040.01	(8.75)	367919.54	(17.45)	11050.55	(0.72)
mRNAs (antisense)**	8445.09	(2.11)	314185.73	(14.90)	1261.43	(0.08)
Overlapping mRNAs**	3761.49	(0.94)	19111.64	(0.92)	938.16	(0.06)
Rest	165367.31	(41.31)	262546.95	(12.45)	34335.12	(2.25)

* no tRNA or rRNA matches
** only genes that are part of the YGOB

Table S2. RNA-Seq data from *S. cerevisiae* wild-type, *+AGO1, +DCR1* and *+AGO1*, *DCR1* strains in comparison to the published RNA-Seq data form wild-type *S. castellii* (*1*). Numbers in parenthesis are percent of reads compared to number of non-ncRNA-matching reads.

	S. castellii				***S. cerevisiae***							
	Wild-type 1		**Wild-type 2**		**Wild-type**		***+AGO1***		***+DCR1***		***+AGO1, DCR1***	
Total genome-matching reads *	3913229.00		4594533.00		21962567.00		21265800.00		20855295.00		20573554.00	
Non-ncRNA-matching reads *	3495348.16	(100.00)	4118241.62	(100.00)	21852788.66	(100.00)	21127961.15	(100.00)	20792442.04	(100.00)	20455194.75	(100.00)
AGO1 (3900 nt)			838 (215 reads/kb)	(0.01)	0.00	(<0.01)	126146.00	(0.6)	17.00	(<0.01)	73788 (18920.00 reads/kb)	(0.36)
DCR1 (1833 nt)			332 (181 reads/kb)	(<0.01)	0.00	(<0.01)	0.00	(<0.01)	21626.00	(0.10)	8108.00 (442.35 reads/kb)	(0.04)
L-A	_		_		107.00	(<0.02)	117.00	(<0.01)	63.00	(<0.01)	156.00	(<0.01)
L-BC	_		_		25.00	(<0.01)	73.00	(<0.01)	15.00	(<0.01)	29.00	(<0.01)
M	_		_		154329.83	(0.71)	372274.57	(1.76)	181836.36	(0.87)	166297.42	(0.81)
Ty (sense)	8574.92	(0.25)	10740.60	(0.26)	327752.72	(1.50)	443101.06	(2.10)	357701.77	(1.72)	140602.38	(0.69)
Ty (antisense)					13277.22	(0.06)	24404.70	(0.12)	12700.57	(0.06)	12930.94	(0.06)
Y' elements (sense)	495.08	(0.01)	571.05	(0.01)	18805.24	(0.09)	95499.92	(0.45)	16701.87	(0.08)	26933.32	(0.13)
Y' elements (antisense)					1596.74	(0.01)	1635.73	(0.01)	1191.84	(0.01)	659.04	(<0.01)
mRNAs (sense)**	3168432.30	(90.65)	3723870.95	(90.42)	19732598.36	(90.30)	17845733.43	(84.47)	18366890.56	(88.33)	18111329.69	(88.54)
mRNAs (antisense)**	17771.69	(0.51)	20554.32	(0.50)	158119.28	(0.72)	335018.63	(1.59)	181812.54	(0.87)	236298.35	(1.16)
Overlapping mRNAs**	172296.29	(4.93)	207809.38	(5.05)	553725.28	(2.53)	462835.41	(2.19)	630612.40	(3.03)	650218.80	(3.18)
Rest	127192.88	(3.64)	154110.31	(3.74)	892451.99	(4.02)	1421121.69	(6.73)	1021273.13	(4.91)	1027843.81	(5.02)

* excluding all reads matching to rRNAs and tRNAs

** using only YGOB annotated genes

Table S3. No evidence for Ago1 homologs from high-throughput genomic sequencing of *Z. bailii* and *H. uvarum*, the two budding-yeast species outside of the *sensu stricto* clade in which dsRNA killer viruses have been described (*20, 28*, *44*). Estimates of genome size are from previous reports (*37, 38*, *43*). The average fraction of conserved proteins of the *Saccharomyces* complex (fig. S1) found within the assembled contigs using tblastn ($E \leq 10^{-5}$) (table S4) is reported as the presence of conserved proteins. The presence or absence of a significant alignment to the indicated Ago1 protein is indicated (parentheses, smallest *E* value). As a control, *S. castellii* was sequenced, and contigs were analyzed in parallel to those of the newly sequenced genomes. To simulate the potentially lower coverage of the *H. uvarum* genome, 1000 cohorts were randomly generated to each include 47% of the *S. castellii* sequences (a percentage chosen so that the fraction of conserved proteins identified by using each cohort approximated that identified from the *H. uvarum* contigs), and the number of cohorts in which an Ago1 homolog was identified is shown.

To test whether *Z. bailii* and *H. uvarum* have the RNAi pathway, we sequenced their genomes using Illumina shotgun sequencing. Within our assemblies, searches that uncovered homologs to most proteins conserved in budding yeast found no homologs of Ago1, whereas repeating the genomic sequencing and analyses with *S. castellii* as a positive control found Ago1 with high confidence, even when simulating lower coverage by restricting analyses to subsets of reads. Thus, as predicted, RNAi was not found in yeast species with dsRNA killer viruses.

			S. castellii	
Species	*Z. bailii*	*H. uvarum*	All reads	Cohorts
Previously estimated genome size	7.7 Mb	~ 11 Mb	~ 10 Mb	~ 10 Mb
Sequence coverage	35 x	37 x	16 x	7.5 x
Total contig length	10.7 Mb	7.9 Mb	9.8 Mb	3.6 Mb
Presence of conserved proteins	98.4%	73.9%	96.0%	71.6%
Alignment to *K. polysporus* Ago1	No (2.2)	No (1.7)	Yes (10^{-39})	1000 of 1000
Alignment to *C. albicans* Ago1	No (2.2)	No (>10.0)	Yes (10^{-22})	848 of 1000

Table S4. Ability to identify homologs of yeast proteins in the two newly sequenced genomes. *H. uvarum, Z. bailii* and *S. castellii* contigs were aligned to proteins of yeasts from the *Saccharomyces* complex. The coverage of the sequenced genomes was assessed by using tblastn (*E* value cutoff 10^{-5}) to search the assembled contigs for homologs of all proteins (all) or proteins conserved among 11 different yeasts of the *Saccharomyces* complex (conserved). Protein sequences were downloaded from the YGOB. The lower yield of predicted proteins in the *H. uvarum* contig set could be due to a lower coverage of the genome or to a more diverged genome of *H. uvarum*, which is an outgroup to the 11 yeasts of the *Saccharomyces* complex (*12*) (fig. S1).

			H. uvarum				*Z. bailii*				*S. castellii*				1000 subsets	
			All		Conserved		All		Conserved		All		Conserved		Conserved	
Species	All	Cons.	Pred.	%	Pred.	%	Pred.	%	Pred.	%	Pred.	%	Pred.	%	Pred.*	%
Ashbya gossypii	4748	3794	3238	68.20	2754	72.59	4428	93.26	3705	97.65	4170	87.83	3556	93.73	1550	40.86
Candida glabrata	5232	4133	3595	68.71	3047	73.72	4876	93.20	4041	97.77	3878	74.12	3943	95.40	2985	72.24
Kluyveromyces lactis	5134	3794	3464	67.47	2801	73.83	4685	91.25	3709	97.76	4387	85.45	3559	93.81	2571	67.76
Kluyveromyces polysporus	5526	4220	3700	66.96	3149	74.62	5039	91.19	4157	98.51	4970	89.94	4055	96.09	3093	73.30
Kluyveromyces waltii	10888	3794	4140	38.02	2779	73.25	6477	59.49	3730	98.31	5746	52.77	3589	94.60	2631	69.35
Kluyveromyces thermotolerans	5171	3794	3488	67.45	2811	74.09	4816	93.13	3741	98.60	3892	75.27	3621	95.44	2684	70.76
Saccharomyces bayanus	5272	4236	3614	68.55	3140	74.13	4954	93.97	4164	98.30	4859	92.17	4095	96.67	3205	75.65
Saccharomyces castellii	5746	4310	3935	68.48	3177	73.71	5365	93.37	4219	97.89	5719	99.53	4300	99.77	4044	93.83
Saccharomyces cerevisiae	6604	4275	3900	59.06	3183	74.46	5510	83.43	4214	98.57	5038	76.29	4141	96.87	3248	75.97
Saccharomyces kluyvery	5406	3794	3594	66.48	2807	73.99	4977	92.06	3756	99.00	4735	87.59	3666	96.63	2775	73.14
Zygosaccharomyces rouxii	5047	3794	3447	68.30	2808	74.01	4976	98.59	3784	99.74	4572	90.59	3685	97.13	2822	74.38

* Average

Table S5. Conditions for phenotypic profiling presented in figures S2 and S8.

	Concentration	
Condition	***S. cerevisiae***	***S. castellii***
Alpha factor	10 μM	10 μM
Anisomycin	30 μM	30 μM
Arabinose	2 %	2 %
Benomyl	15 μM	15 μM
Cadmium chloride	0.8 μM	0.16 μM
Caffeine	2 mM	2 mM
Cerulenin	0.44 μM	0.44 μM
Cetylpyridinium chloride	0.776 μM	0.776 μM
Chlorhexidine	2.71 μM	2.71 μM
Chlorpromazine	15.7 μM	15.7 μM
Clotrimazole	0.483 μM	0.483 μM
Cobalt chloride	1.2 mM	0.12 mM
Copper sulfate	180 μg/mL	180 μg/mL
Cyclosporin A	100 μg/mL	100 μg/mL
Doxorubicin	21.6 μM	21.6 μM
Ethanol	5 %	5 %
Ethanolamine	2 mM	2 mM
Ferric chloride	2.5 mM	2.5 mM
Fluconazole	16 μg/mL	16 μg/mL
Flufenamic acid	1 mM	1 mM
Galactose	2 %	2 %
Gliotoxin	100 ng/mL	100 ng/mL
Glucose	2 %	2 %
Glycerol	2 %	2 %
Guanidinium hydrochloride	5 mM	5 mM
Ibuprofen sodium salt	50 μM	50 μM
Lactose	2 %	2 %
Latrunculin B	12.6 μM	12.6 μM
Lidocaine	5 mg/mL	5 mg/mL
Lithium chloride	200 mM	200 mM
Magnesium chloride	150 mM	150 mM
Manganese chloride	10 mM	10 mM
Mannose	2 %	2 %
Menadion	29 μM	29 μM
Neomycin	100 μM	100 μM
Nickel chloride	500 μM	50 μM
Novobiocin	1 mM	1 mM
Oxolinic acid	50 μM	50 μM
Paromomycin	500 μM	500 μM
Pentachlorophenol	31.7 μM	3.17 μM
Promethazine	20 μM	20 μM
Propiconazole	16 μg/ml	16 μg/ml
Quercetin	4 μM	4 μM
Raffinose	2 %	2 %
Resveratrol	10 μM	10 μM
Sodium chloride	0.5 M	0.5 M
Staurosporine	4 μg/mL	4 μg/mL
Triflouperazine	5 μM	5 μM
Tunicamycin	0.296 μM	0.296 μM
Zinc chloride	5 mM	500 μM

Table S6. Strains used and generated in this study.

Strain	Genotype	Species	Reference
DPB249	*MAT*a *leu2-3,112 trp1-1 can1-100 ura3::EGFP(S65T)-KanMX6 ade2-1 his3-11,15*	*S. cerevisiae* W303-1b	*(1)*
DPB252	*MAT*a *leu2-3 TRP1::pTEF-Ago1 can1-100 ura3::EGFP(S65T)-KanMX6 ade2-1 his3-11,15*	*S. cerevisiae* W303-1b	This study
DPB255	*MAT*a *LEU2::pTEF-Dcr1 trp1-1 can1-100 ura3::EGFP(S65T)-KanMX6 ade2-1 his3-11,15*	*S. cerevisiae* W303-1b	*(1)*
DPB258	*MAT*a *LEU2::pTEF-Dcr1 TRP1::pTEF-Ago1 can1-100 ura3::EGFP(S65T)-KanMX6 ade2-1 his3-11,15*	*S. cerevisiae* W303-1b	*(1)*
DPB040	*MAT*a *LEU2::pTEF-Dcr1 TRP1::pTEF-Ago1 ago1Δ:HYG can1-100 ura3::EGFP(S65T)-KanMX6 ade2-1 his3-11,15*	*S. cerevisiae* W303-1b	This study
DPB041	*MAT*a *LEU2::pTEF-Dcr1 TRP1::pTEF-Ago1 ago1Δ:HYG can1-100 ura3::EGFP(S65T)-KanMX6 ade2-1 his3-11,15*	*S. cerevisiae* W303-1b	This study
NCYC 2600	Wild-type	*S. paradoxus* NCYC 2600	*(31)*
CBS8840	Wild-type	*S. kudriavzevii* CBS8840	*(27)*
IFO 1815	Wild-type	*S. mikatae* IFO 1815	*(27)*
IFO 1816	Wild-type	*S. mikatae* IFO 1816	*(45)*
Y235	*MAT*a*/MATa ura3-1/ura3-1*	*S. castellii* CBS4310	NCYC
DPB005	*MAT*a *ura3-1 hoΔ*	*S. castellii* CBS4310	*(1)*
DPB007	*MAT*a *ura3-1 hoΔ ago1Δ*	*S. castellii* CBS4310	*(1)*
DPB009	*MAT*a *ura3-1 hoΔ dcr1Δ*	*S. castellii* CBS4310	*(1)*
F2037	Wild-type	*S. castellii* CBS4309	*(37)*
EY1698	Wild-type	*C. glabrata* EY1698	*(32)*
412	Wild-type	*Z. bailii* 412	*(20)*
KpolWT	Wild-type	*K. polysporus* DSM70294	*(33)*
NCYC2644	Wild-type	*K. waltii* NCYC 2644	*(34)*
NRRL 12651	Wild-type	*S. kluveryi* NRRL 12651	*(35)*
CliB 209	Wild-type	*K. lactis* CliB 209	*(36)*
470	Wild-type	*H. uvarum* 470	*(28)*
ATCC 32356 (75 (44-2))	*a2bk*	*U. maydis*	*(22)*
ATCC 32357 (77 (45-2))	*a1bM*	*U. maydis*	*(22)*
ATCC 32599 (car-4)	offspring of car-1 x car-2	*U. hordei*	*(39)*
ATCC 34038 (l4)		*U. hordei*	*(40)*
U807	*MAT-1*	*U. hordei*	*(29)*
Uh364	*MAT-1*	*U. hordei*	*(41)*
U809	*MAT-1*	*U. hordei*	*(29)*
Uh112	*MAT-1, adeΔ*	*U. hordei*	*(30)*
Uh362	*MAT-2*	*U. hordei*	*(41)*
Uh100	*MAT-2, adeΔ*	*U. hordei*	*(30)*